BRITISH GEOLOGICAL SURVEY

TECHNICAL REPORT

Mineralogy & Petrology Series

REPORT NO. WG/99/24C

MINERALOGICAL AND PETROGRAPHICAL CHARACTERISATION OF A 1 m CORE FROM THE UTSIRA FORMATION, CENTRAL NORTH SEA

J.M. Pearce, S.J. Kemp and P.D. Wetton

Date
May 11, 2000
Classification
Commercial-in-confidence
Geographical index
Norwegian Sector, Central North Sea
Subject index
Utsira Formation, Miocene, sandstone, CO_2 disposal

Bibliographic reference
Pearce, J.M., Kemp, S.J. and Wetton, P.D. 1999. Mineralogical and petrographical characterisation of a 1m core from the Utsira Formation, Central North Sea.

© NERC 1999 British Geological Survey, Keyworth, Nottingham NG12 5GG,

EXECUTIVE SUMMARY

A 1 m length of frozen core from the Utsira Formation of Well 15/9-A-23 (1085 m to 1086 m), Viking Graben, Central North Sea, has been mineralogically and petrographically characterised as part of Subtasks 1.1. and 1.3. of the Saline Aquifer CO_2 Storage (SACS) project. The analyses involved mineralogical characterisation by X-ray diffraction (XRD) analysis, petrographic analysis by secondary scanning electron microscopy (SEM) including backscattered scanning electron microscopy (BSEM), and limited electron probe microanalyses (EMPA) of selected minerals. Four subsamples were examined by a combination of these techniques to assess the mineralogical and petrographical variations of the Utsira Formation at the sub-1 m scale.

The Utsira Formation is a mixed sandstone and mudstone formation. It forms part of the Nordland Group. It is Miocene to early Pliocene in age, and found in the Viking Graben. The type section, in Norwegian well 16/1-1, contains at its base a very clean, highly porous and permeable sand approximately 160 m thick. This sand body is referred to in the SACS project as the Utsira Sand. It forms the CO_2 storage reservoir at Sleipner.

The Utsira Sand lies a short way above the major 'Mid-Miocene' onlap surface and was deposited in the centre of the basin. In the Sleipner area, its top occurs at 750 m to 800 m vertical depth and it is 150 m to 250 m thick. It is overlain by a regional shale drape which acts as a cap rock, and above this by Pliocene progradational clayey and silty sediments derived from both Scandinavia and the Scotland-Shetland area. It consists of medium to fine grained, highly permeable sand with microfossil fragments. Due to the presence of glauconite and abundant fossil fragments, it has been suggested that the Utsira Sand was deposited in shallow marine conditions. However, its location in the basin centre and the presence of mixed shallow marine and outer shelf-dwelling microfossils suggests that it may represent a basin floor fan.

The sandstone is a medium grained, moderately to well sorted, very poorly cemented and friable subarkosic sand. It comprises predominantly quartz with minor plagioclase, K-feldspar, calcite (probably shell fragments) and common bioclastic debris including foraminifera, radiolaria and sponge spicules. Some detrital grains are covered in a thin, <10 µm, clay coating which XRD indicates comprises mainly smectite with minor illite and chlorite. SEM evidence suggests that some smectite morphologies could be indicative of authigenic development. Pyrite is a minor but commonly distributed authigenic mineral occurring as framboidal aggregates, especially within foraminifera tests. The most notable diagenetic modification is the development of minor amounts

of two zeolites, phillipsite and clinoptilolite. Phillipsite is the dominant zeolite. Both zeolites have developed through precipitation directly from porewaters, with the dissolution of radiolaria and sponge spicules providing a likely source of biogenic silica. Although common, the zeolites only form a very small component of the sand and do not represent a significant modification to porosity and permeability.

CONTENTS

Page

1. INTRODUCTION **1**

2. LABORATORY METHODS **2**
2.1. Sample preparation **2**
2.2. X-ray diffraction analysis **2**
2.2.1. Qualitative analysis 2
2.2.2. Zeolite speciation 3
2.2.3. Whole-rock quantitative analysis 4
2.2.4. XRD profile modelling 5
2.3. Scanning electron microscopy **5**
2.4. Modal analysis **5**

3. RESULTS **6**
3.1. Whole-rock analysis **6**
3.2. Clay mineral analysis **7**
3.3. Petrographic results **8**

4. DISCUSSION **10**

5. SUMMARY **10**

6. REFERENCES **12**

TABLES

Table 1: Summary of the whole-rock mineralogy of the Utsira Formation samples. 6
Table 2: Summary of <2 µm clay mineral X-ray diffraction analyses for the Utsira Formation samples 7
Table 3. Summary of 'light' 2-30 µm X-ray diffraction analyses for the Utsira Formation samples 8
Table 4: Modal mineralogical composition of the Utsira Formation, 1085 to 1086 m. 9

FIGURES

Figure 1: 1 m sandstone core from the Utsira Formation, well 15/9-A-23. 15
Figure 2: Schematic plan of the 1 metre core identifying sample locations. 16
Figure 3: Schematic flowsheet describing the modal analysis methodology employed. 17
Figure 4: Whole-rock X-ray diffraction traces for samples E641A (black trace), E642 (red trace), E643 (magenta trace) and E644 (blue trace) showing major peak assignations and d spacings. Co-Ka radiation. 18
Figure 5: <2 µm oriented mount X-ray diffraction traces (air-dry: black trace; glycol-solvated; red trace, heated 550°C/2 hours; magenta trace) for samples E641A (above) and E642 (below) showing identified minerals and their diagnostic d spacings. Co-Kα radiation. 19
Figure 6: <2 µm oriented mount X-ray diffraction traces (air-dry: black trace; glycol-solvated: red trace, heated 550°C/2 hours; magenta trace) for samples E643 (above) and E644 (below) showing identified minerals and their diagnostic d spacings. Co-Kα radiation. 20

Figure 7: XRD Trace of -30+2 µm 'light' fraction, indicating clinoptilolite and phillipsite. 21

PLATES

Plate 1: Moderately to well sorted, subrounded to subangular, fine to medium grained sandstone of the Utsira Formation. Well 15/9-A-23, 1085 to 1086 m. E643S1/05. 21

Plate 2: Moderately to well sorted, subrounded to subangular, fine to medium grained sandstone of the Utsira Formation with shell and foraminifera fragments. Well 15/9-A-23, 1085 to 1086 m. E641P1/02. 21

Plate 3: Rare siliceous sponge spicule. Well 15/9-A-23, 1085 to 1086 m. E641S3/11. 21

Plate 4: Typical examples of altered biotite (bottom) and muscovite flakes. Collophane is developing along the basal cleavages of the biotite. Well 15/9-A-23, 1085 to 1086 m. E641P1/04. 21

Plate 5: Typical example of rare glauconite grain that is partially replaced by collophanic material (towards top of grain) and pyrite along radial cracks. Well 15/9-A-23, 1085 to 1086 m. E641P1/03. 21

Plate 6: Rare framboidal pyrite aggregate. Well 15/9-A-23, 1085 to 1086 m. E642S2/02. 21

Plate 7: A foraminifera test (bottom centre) with authigenic framboidal pyrite precipitating within cavities and a sponge spicule (top centre). Well 15/9-A-23, 1085 to 1086 m. E641P1/06. 22

Plate 8: Typically corroded detrital albite grain. Well 15/9-A-23, 1085 to 1086 m. E643S1/01. 22

Plate 9: Authigenic prismatic phillipsite crystals developing on a calcite substrate. Well 15/9-A-23, 1085 to 1086 m. E641S3/05. 22

Plate 10: Detailed view of authigenic phillipsite prism developing into open void. Well 15/9-A-23, 1085 to 1086 m. E641S3/06. 22

Plate 11: Euhedral, authigenic, rhombohedral clinoptilolite blocking a pore throat. Well 15/9-A-23, 1085 to 1086 m. E641S3/03. 22

Plate 12: Euhedral authigenic clinoptilolite forming overgrowths to tentatively identified corroded feldspar. Well 15/9-A-23, 1085 to 1086 m. E641S3/04. 22

Plate 13: Rare, interpenetrant form of phillipsite. Well 15/9-A-23, 1085 to 1086 m. E641S3/02. 23

Plate 14: Authigenic, poikilotopic clinoptilolite cements detrital quartz and feldspar grains. Note authigenic micron-scale pyrite (bright specks) also enclosed by clinoptilolite. Well 15/9-A-23, 1085 to 1086 m. E641P1/01. 23

1. INTRODUCTION

A 1 m length of frozen core (Figure 1) from the Utsira Formation of Well 15/9-A-23 (1085 to 1086 m), Viking Graben, North Sea, has been mineralogically and petrographically characterised as part of Subtasks 1.1. and 1.3. of the Saline Aquifer CO_2 Storage (SACS) project. The analyses involved mineralogical characterisation by X-ray diffraction (XRD), petrographic analysis by scanning electron microscopy (SEM) including backscattered scanning electron microscopy (BSEM), and limited electron probe microanalyses (EMPA) of selected minerals. Four subsamples were examined by a combination of these techniques to assess the mineralogical and petrographical variations of the Utsira at the sub-1 m scale (Figure 2).

The Utsira Formation consists of a mixture of sandstone and mudstone. It forms part of the Nordland Group Group (Deegan and Scull, 1977) It is of Miocene to early Pliocene age (Isaksen and Tonstad, 1989) and is found in the Viking Graben. The type section, in Norwegian well 16/1-1, contains at its base a thick very clean sand approximately 160 m thick. This sand body is referred to in the SACS project as the Utsira Sand. It forms the CO_2 storage reservoir at Sleipner.

The Utsira Sand lies a short way above the major 'Mid-Miocene' onlap surface and was deposited in the centre of the basin. In the Sleipner area its top occurs at 750 m to 800 m vertical depth and it has a thickness of 150 m to 250 m. It is overlain by a regional shale drape which acts as a cap rock, and above this by Pliocene progradational clayey and silty sediments derived from both Scandinavia and the Scotland-Shetland area. It consists of medium to fine grained, highly permeable sand with microfossil fragments. Due to the presence of glauconite and abundant fossil fragments, it has been suggested that the Utsira Sand was deposited in shallow marine conditions (Isaksen and Tonstad, 1989; Rundberg, 1989). However, its location in the basin centre and the presence of mixed shallow marine and outer shelf-dwelling microfossils suggests that it may represent a basin floor fan (Gregersen et al., 1997; Gregersen, 1998).

The sediments may have been derived from the uplift and erosion of 400-600 m of Neogene sediments off south-west Norway (Ghazi, 1992; Hansen, 1996) or from 1500 m of uplift and erosion in the west Norwegian mountains (Doré, 1992; Riis and Fjeldskaar, 1992).

2. LABORATORY METHODS

2.1. Sample preparation

The contamination of the core by infiltration of drilling mud into the saline porewaters resulted in the extensive precipitation of potassium chloride (?sylvite) and halite crystals. Washing the core to remove this contamination was not possible due to its very friable nature. On receipt, the subsamples for XRD were dried at 55°C. For whole-rock analysis, a representative portion was removed and hammer-milled to a grain size of <120 µm. Approximately 5 g of the hammer-milled material was sub-sampled and wet-micronised under acetone for 10 minutes.

A further 35 g (approximately) portion of each dried sample was placed in a plastic bottle with approximately 200 ml distilled water and shaken on a reciprocal shaker for 2 hours. Further dispersion was achieved by treating the samples with ultrasound before wet-seiving to pass a 63 µm mesh. The >63 µm material (the ‘sand’ fraction) was dried at 55°C and bagged. The <63 µm suspended material was placed in a 250 ml measuring cylinder with 1 ml 0.1M sodium hexametaphosphate ('Calgon') solution to disperse the individual clay particles and prevent flocculation. After standing for a period dictated by Stokes' Law, a nominal <2 µm (‘clay’) fraction was removed, dried at 55°C and bagged. The remaining 2-63 µm (‘silt’ fraction) material was also dried at 55°C and bagged.

For SEM analysis small chips were removed from the frozen core by hammer and chisel and freeze-dried in an Edwards Modulyo freeze drier for approximately 24 hours. A freshly fractured surface was then produced and the specimen mounted on Al pin-type stubs using Leit-C carbon cement. The specimens were then coated in a thin layer of carbon approximately 25 nm thick in an Emitech carbon evaporation coater. Polished thin sections were also produced from freeze-dried subsamples following blue-dyed resin impregnation. Polished thin sections were coated in a thin layer of carbon, approximately 25 nm thick, in an Emitech carbon evaporation coater.

2.2. X-ray diffraction analysis

2.2.1. Qualitative analysis

The micronised powders were back-loaded into aluminium sample holders for whole-rock XRD analysis. XRD analyses were carried out using a Philips PW1700 series automatic diffractometer equipped with a cobalt target X-ray tube and operating at 45 kV and 40 mA. Diffraction data were analysed using Philips X’Pert© software coupled to an International Centre for Diffraction Data

(ICDD) database running on a Gateway personal computer system. Whole-rock samples were scanned from 3-50 °2θ at a scanning speed of 0.48 °2θ/minute.

In order to identify the clay minerals present in the sandstone samples, oriented mounts were prepared and examined as air-dry and glycol-solvated mounts and after heating to 550°C for 2 hours. Oriented mounts were prepared by re-suspension of 100 mg of the <2 µm material in a minimum of distilled water before pipetting onto a ceramic tile in a vacuum apparatus. Ethylene glycol-solvation of the oriented mounts was achieved by placing the samples in a desiccator filled with the reagent and heating to 55°C overnight. The oriented mounts were scanned from 2-32 °2θ at 0.48 °2θ/minute.

2.2.2. Zeolite speciation

Routine clay mineral XRD analysis suggested that the Utsira Formation sandstones contain traces of zeolite-group minerals. However, due to their low concentrations, it proved impossible to identify the zeolites more precisely. Subsequent petrographic analysis revealed that the zeolite occurs as fine-grained (<20 µm) crystals but in two different forms. Most common are elongate, prismatic laths but also present is a rarer, tabular rhombohedral form.

In order to speciate the zeolites, it was therefore decided to separate and concentrate the zeolite following the method of Ming and Dixon (1987). Approximately 35 g of each dried sample was placed in a plastic bottle with approximately 200 ml distilled water and shaken on a reciprocal shaker for 2 hours. Further dispersion was achieved by treating the samples with ultrasound before wet-sieving to pass a 63 µm mesh. The >63 µm material (the ‘sand’ fraction) was discarded. The <63 µm suspended material was placed in a 250 ml measuring cylinder with 1 ml 0.1M sodium hexametaphosphate ('Calgon') solution to disperse the individual clay particles and prevent flocculation.

After standing for a period determined from Stokes' Law, the >30 µm material was removed and discarded. The measuring cylinder was then topped up with deionised water and the process repeated until no further >30 µm material was discernible. The remaining <30 µm material was then stirred and allowed to stand before removing and discarding a nominal <2 µm fraction. This process was again repeated until no further <2 µm material was discernible. The remaining 2-30 µm fraction was then dried at 55 °C and stored in glass vials.

In order to concentrate any zeolites in the 2-30 µm separate, the samples were then processed using a heavy liquid separation method (Ming and Dixon, 1987). Approximately 0.5 g of the 2-30 µm separates were placed in a 40 ml centrifuge tube and ultrasonically dispersed in a heavy

liquid of bromoform, adjusted to a specific gravity of 2.3. Once dispersed, the tubes were centrifuged at 2000 rpm for 5 minutes and the 'light' (containing any zeolites) and 'heavy' fractions isolated by pouring through filter papers. Both fractions were washed several times with acetone to remove any remaining heavy liquid residue.

The identity of the mineral separate was determined by XRD. Material for XRD was prepared by grinding a few milligrams of the 'light' 2-30 µm fraction to a powder in an agate pestle-and-mortar and deposited on a 'zero-background' silicon substrate using a single drop of acetone.XRD analyses were carried out under the same conditions as described in Section 2.2.1.

2.2.3. Whole-rock quantitative analysis

Modal mineralogy of the samples was determined by quantitative XRD analysis following the internal standard method (Brindley & Brown, 1980). The XRD equipment was calibrated using a batch of standards containing appropriate mineral concentrations that simulated the mineral assemblage of the sandstones. These included a known proportion of corundum (α-Al2O3, National Institute of Standards and Technology reference material no.674a) to act as an internal standard together with differing proportions of quartz, albite, orthoclase, calcite, aragonite and muscovite. In order to thoroughly homogenise the mineral mixtures, the powders were micronised for five minutes under acetone.

Suitable peak parameters were selected by comparison of standard mineral diffraction traces with ICDD standards held on computer disk. Generally the most intense peak for each mineral was selected, in order to produce the lowest possible detection limit. In the case of the feldspars, whose diffraction traces present many peaks, distinct isolated peaks were not available and for this reason the feldspar data should be treated with caution. In addition the solid-solution prevalent in the feldspars leads to small changes in diffraction patterns which cannot be resolved by employing single species standards. Similarly, the 10Å peak chosen to quantify micas actually represents a range of species from biotite and muscovite to illite and illite/smectite. The undifferentiated term 'mica' is therefore employed for the concentration obtained from the 10Å peak.

Slow scans were made over the each of the selected peaks (one for each mineral phase including corundum) and individual calibration curves were produced for the mean ratio:

$$\text{Peak area}_{\text{mineral}} / \text{Peak area}_{\text{corundum}}$$

The Utsira Formation samples were spiked with 10% corundum, homogenised and scanned by the same analysis program. Normalised mean mineral concentrations were produced using the standard calibration curves. Errors for the quoted mineral concentrations have a probable accuracy of ±5% for quartz, calcite and aragonite. Higher errors are likely for the quoted 'mica' and feldspar concentrations.

2.2.4. XRD profile modelling

In order to gain further information about the nature of the clay minerals present in the samples, modelling of XRD profiles was carried out using Newmod-for-Windows™ (Reynolds & Reynolds, 1996) software.

Modelling was also used to assess the relative proportions of clay minerals present in the <2 µm fractions by comparison of sample XRD traces with Newmod-for-Windows™ modelled profiles. The modelling process requires the input of diffractometer, scan parameters and a quartz intensity factor (instrumental conditions) and the selection of different sheet compositions and chemistries. In addition, an estimate of the crystallite size distribution of the species may be determined by comparing peak profiles of calculated diffraction profiles with experimental data. By modelling the individual clay mineral species in this way, mineral reference intensities were established and used for quantitative standardization following the method outlined in Moore & Reynolds (1997).

2.3. Scanning electron microscopy

The stubs and polished thin sections were examined on a Leo 435VP scanning electron microscope fitted with a solid-state four element backscattered electron detector. Qualitative mineral identification was facilitated by an Oxford Instruments ISIS 300 energy dispersive X-ray microanalyser.

2.4. Modal analysis

The modal composition of the samples was estimated using a petrographic image analysis method. The method uses BSEM images generated by a scanning electron microscope (SEM) and energy-dispersive X-ray analysis (EDXA) data to identify the minerals present. Using a list of minerals drawn up during petrographic analysis, a sequence of logical comparisons and image processing operations are defined to allow all minerals present to be uniquely identified. The area

occupied by each mineral, as well as porosity, can then be determined for a series of BSEM images across the specimen. The modal analysis is estimated by averaging the mineral data obtained from each image. A simplified flowsheet of the analysis procedure is shown in Figure 3. The Mineral Series binary maps represent groups of minerals which have similar BSE characteristics. These are processed in turn using EDXA data to extract the individual minerals.

The number of fields required to obtain statistically valid data, is calculated using the following formula,

$$N = \left[k.\frac{s}{\varepsilon} \right]^2$$

N - number of fields
k - confidence interval @ 95 % (1.96)
s - standard deviation of the mineral phase estimates from each field of view
ε– permitted error in modal estimate for selected mineral phase

In this study the 'number of fields' calculation was made using the quartz data, as this was present in every image field, with a permitted error of ± 2 modal%. Modal analysis was performed using a Carl Zeiss Vision (formerly Kontron Elektronik) KS400 Image Analysis system and SEM Processor. SEM operating conditions of 20 kV accelerating voltage and 4 nA probe current were used.

3. RESULTS

3.1. Whole-rock XRD analysis

The samples present a very similar whole-rock mineralogy and are predominantly composed of quartz with minor K-feldspar and traces of albite, calcite, aragonite and undifferentiated mica species (Figure 4).

Table 1: Summary of the whole-rock mineralogy of the Utsira Formation samples.

Sample	Quartz	Calcite	K-feldspar	% mineral Albite	Aragonite	'Mica'
E641A	75	2	14	3	3	3
E642	75	3	13	3	3	3
E643	75	2	14	3	3	3
E644	76	3	12	3	4	3

3.2. Clay mineral analysis

On dispersion, it was noticed that all the core samples contain a ?detergent or ?surfactant (probably as a drilling mud additive) which caused the suspensions to froth.

In order to provide quantitative clay mineralogical data for the Utsira Formation samples, peak integration was performed on the smectite d001 (approximately 17Å), illite d002 (approximately 5Å) and chlorite d002 (7.1Å) reflections on the glycol-solvated traces. These are the most suitable reflections available as they are relatively close together and therefore minimise geometry and sample thickness effects. Sample peak areas were then compared with those derived from modelling the individual clay mineral species with Newmod-for-Windows™ software and normalised to 100%. The results of <2 µm quantitative clay mineralogical analyses are summarised in Table 2.

Table 2: Summary of <2 µm clay mineral X-ray diffraction analyses for the Utsira Formation samples

Sample	Smectite	Illite	Chlorite
E641A	59	27	14
E642	64	23	12
E643	73	18	8
E644	71	20	9

The clay mineralogy of the samples appears generally uniform and is predominantly composed of smectite with minor amounts of illite and chlorite. Small quantities of kaolinite may also be present but could not be distinguished in the presence of chlorite (Figures 5 and 6).

Newmod-for-Windows™ modelling of the smectite identified in the samples indicates a mean defect-free distance of 1 layer and a crystallite-size range of 1 to > 2 layers.

The illite in all the samples shows very restricted ‘swelling’ on glycol-solvation, exhibited by a slight sharpening of its basal XRD reflections, which may represent the presence of very few (possibly <2%) smectite interlayers. Newmod-for-Windows™ modelling indicates that the illite contains 0.7 K; 0.05 Fe per $(Si, Al)_4O_{10}(OH)_2$ and a mean defect-free distance of 14 layers and a crystallite-size range of 1 to > 40 layers.

Peak intensity ratios (d_{001}/d_{002}) indicate that the chlorite present in the samples is a relatively Fe-rich species. Heat treatment to 550°C for 2 hours collapses the d_{002}, d_{003} and d_{004} chlorite spacings

but intensifies the d_{001} peak. Modelling indicates a mean defect-free distance of 8 layers and a crystallite-size range of 1 to > 26 layers.

XRD analysis also indicates that the <2 µm fraction of all four samples also contains substantial quantities of cristobalite, quartz and aragonite. A low intensity peak at c.8.98Å (Figures 5 and 6) may also indicate the presence of a zeolite mineral, possibly clinoptilolite.

As shown in Table 3, XRD analysis reveals that the combination of gravity and heavy liquid separation has successfully concentrated the zeolites present in the Utsira Formation sandstones. The 'light' fraction of all four 2-30 µm separates are dominated by the zeolites clinoptilolite [$(Na, K, Ca)_6(Si, Al)_{36}O_{72}.20H_2O$] and phillipsite [$K_2Ca_2(Al, Si)_{16}O_{32}.13.5H_2O$] with subordinate amounts of quartz and calcite.

Table 3: Summary of 'light' 2-30 µm X-ray diffraction analyses for the Utsira Formation samples

Sample	Zeolite minerals	Other minerals
E641A	Clinoptilolite, phillipsite	-
E642	Clinoptilolite, phillipsite	Quartz, calcite
E643	Clinoptilolite, phillipsite	Quartz, calcite
E644	Clinoptilolite, phillipsite	Quartz, calcite

Figure 7 shows the XRD trace obtained from the 'light' 2-30 µm fraction of sample E642 compared to the ICDD 'stick' patterns for clinoptilolite and phillipsite.

3.3. Petrographic results

The Utsira Formation sandstone comprises a poorly cemented, fine to medium grained, moderately sorted sand (Plate 1). It is composed (Table 4) predominantly of subangular to subrounded, occasionally angular, quartz grains with minor K-feldspar, plagioclase, calcite (Plate 2) and coarse sand- to gravel-sized shell fragments including siliceous sponge spicules (Plate 3), foraminifera and radiolarian tests. Rare biotite flakes are splayed at their edges along basal cleavages (Plate 4). Clay-grade material is rare, except for minor detrital clay coatings on some grains, typically up to 10 µm thick. Rare glauconitic grains are present (Plate 5), which are typically partially replaced by collophanic material and pyrite. Rare heavy minerals include fine, subrounded, ilmenite, zircon, garnet, apatite and rutile grains.

Table 4: Modal mineralogical composition of the Utsira Formation, 1085 to 1086 m.

Phase	Volumetric %		Mineral %
	(Average)	Std. Deviation	(Average)
Quartz	44.19	2.410	76.36
K-feldspar	4.01	1.268	6.92
Plagioclase	1.74	0.228	3.00
Chlorite	0.77	0.217	1.33
Mica	3.02	0.877	5.22
Zeolite	0.13	0.088	0.22
Calcite	3.90	0.707	6.73
Ti Oxides	0.02	0.031	0.04
Apatite	0.01	0.004	0.00
Ilmenite	0.07	0.038	0.11
Pyrite	0.03	0.014	0.05
Porosity	41.99	0.834	-

Approx. 1300 grains analysed

Diagenetic modification includes submicron, sub- to euhedral, pyrite forming framboidal aggregates up to 10 µm across (Plate 6) often developed within foraminifera tests (Plate 7). Rare, irregular clay flakes suggest the presence of smectitic clay in some areas. While it is possible that this smectitic clay may be derived from drilling mud contamination, the lack of sharply defined peaks on XRD traces would appear to preclude this. Plagioclase grains, especially albite grains, are typically etched (Plate 8) and some are further etched to develop minor local secondary porosity with relict, skeletal grains. Aragonite also develops with a rare elongate tabular to rod form and is often etched.

The most significant diagenetic modification is the precipitation of common euhedral, fine grained clinoptilolite and phillipsite (identified by XRD analysis of a specifically separated fraction, Figure 7). SEM, BSEM and EPMA analyses further confirm the authigenic formation of zeolites, typically forming isolated crystals 10-20 µm long lining pore walls. Two morphologies, a common elongate euhedral prismatic lath (Plates 9 and 10) and a rarer tabular, rhombohedral form (Plate 11 and 12) are developed. They are not restricted to one specific mineral substrate but develop from most surfaces. The habit, qualitative chemistry and pseudo-orthorhombic symmetry indicate the prismatic crystals are probably phillipsite and the tabular, rhombohedral forms are clinoptilolite (Mumpton, and Ormsby, 1976). The phillipsite occasionally develops an interpenetrant form (Plate 13). The clinoptilolite is rarely observed in thin section forming a poikilotopic cement (Plate 14) enclosing, and therefore post-dating, the authigenic pyrite. EDXA indicates that both forms have similar chemistry with the exchangeable cations dominated by K and Na, with minor Ca detected in some clinoptilolite crystals.

4. DISCUSSION

Zeolites are common authigenic minerals in marine sediments. Their formation is thought to be influenced by temperature, composition of the host sediment, pore water and mineral precursor (Kastner and Stonecipher, 1978). Clinoptilolite is the most abundant zeolite in marine sediments and occurs in a variety of host sediments from near-surface to several hundreds of metres below the sea floor (Stonecipher, 1978; Gingele & Schulz, 1993). Phillipsite is most abundant in recent to Eocene, clayey to volcanogenic sediments with low sedimentation rates (typically < 5 m 10^{-6} years). Clinoptilolite is generally reported from Cretaceous to Miocene, calcareous and clayey sediments with higher sedimentation rates (> 5 m 10^{-6} years).

Phillipsite is typically interpreted to form from alteration of basaltic glass shards or palagonite (Stonecipher, 1978; Kastner and Stonecipher, 1978). Clinoptilolite is typically associated with the alteration of rhyolitic glass (e.g. Iijiama, 1978, Aoyagi and Kazama, 1980; Ogihara and Iijama, 1989; Ogihara, 1994). However, clinoptilolite has also been observed growing in the interior of radiolarians and foraminifera in sediment with no detectable volcanic material (Berger and von Rad, 1972; Vanucci et al., 1992). This indicates a relationship between biogenic silica and clinoptilolite formation (Nathan and Flexer, 1977; Riech and von Rad, 1979, Bohrman et al. 1989; Gingele and Schulz, 1993). These authors suggest that clinoptilolite precipitates from Si-rich interstitial water with biogenic silica (opal-A) as the main silica source.

No evidence was found that volcanogenic precursors led to the formation of phillipsite or clinoptilolite in the Utsira samples examined in this study. The presence of siliceous sponge spicules and radiolaria in the Utsira provide the required source of porewater silica. However, the source of the aluminium and alkali metals is not yet understood. It is therefore suggested that the phillipsite and clinoptilolite identified here derived from direct precipitation from silica-rich porewaters and not alteration of volcanogenic material.

5. SUMMARY

A 1 m length of sandstone core from the Utsira Formation of Well 15/9-A-23 (1085 m to 1086 m) was received in four broken sections (Figure 1). These were examined by XRD, SEM, BSEM and EPMA techniques to characterise the sandstone mineralogy and petrography (Figure 2). The

sandstone is a medium grained, moderately to well sorted, very poorly cemented and friable subarkosic sand. It comprises predominantly quartz with minor plagioclase, K-feldspar, calcite (probably shell fragments) and common bioclastic debris including foraminifera, radiolaria and sponge spicules. Some detrital grains are covered in a thin, <10 µm, clay coating which XRD indicates comprises mainly smectite with minor illite and chlorite. Although the smectite may be derived from drilling mud, the lack of sharply defined peaks, indicating a crystalline smectite, appears to preclude this. Pyrite is a minor but commonly distributed authigenic mineral occurring as framboidal aggregates, especially within foraminifera tests. The most notable diagenetic modification for the storage of CO_2, is the development of two minor zeolites, phillipsite and clinoptilolite. Phillipsite is the dominant zeolite. Both zeolites have developed through precipitation directly from porewaters with the dissolution of radiolaria and sponge spicules providing a source of biogenic silica. Although common, the zeolites only form a very small component of the sand and do not represent a significant modification to porosity and permeability.

6. REFERENCES

Aoyagi, K. Kazama, T. 1980. Transformational changes of clay minerals, zeolites and silica minerals during diagenesis. *Sedimentology*, **27**, 179-188.

Berger, W.H. and von Rad, u. 1972 Cretaceous and Cenozoic sediments from the Atlantic Ocean. In: Hayes, D.E., Pimm, A.C. et al., *Init Repts., DSDP*, **14**, U.S. Govt. Printing Office, Washington, 787-954.

Bohrman, G. Stewin, R., Faugeres, J-C. 1989 Authigenic zeolites and their relation to silica diagenesis in ODP Site 661 sediments (Leg 108 Eastern Equatorial Atlantic). *Geologische Rundschau*, **78(3)**, 779-792.

Brindley, G W & Brown, G. 1980. *Crystal structures of clay minerals and their X-ray identification*. Mineralogical Society, London.

Deegan, C.E. and Scull, B.J., 1977. A standard lithostratigraphical nomenclature for the central and northern North Sea. Institute of Geological Sciences, London; *Oljedirektoratet, Stavanger report* 77/25, NPD-Bulletin, 1, 35pp.

Doré, A.G., 1992. The Base Tertiary surface of southern Norway and the northern North Sea. *Norsk Geologisk Tidsskrift*, **72**, 259-265.

Ghazi, S.A., 1992. Cenozoic uplift in the Stord Basin area and its consequences for exploration, *Norsk Geologisk Tidsskrift*, **72**, 285-290.

Gingele, F.X. and Schulz, H.D. 1993. Authigenic zeolites in Late Pleistocene sediments of the South Atlantic (Angola Basin). *Marine Geology*, **111**, 121-131.

Gregersen, U., Sørensen, J.C. and Michelsen, O., 1997. Stratigraphy and facies distribution of the Utsira Formation and the Pliocene sequences in the northern North Sea. *Marine and Petroleum Geology*, **14**, 893-914.

Gregersen, U. 1998. Upper Cenozoic channels and fans on 3D seismic data in the northern Norwegian north Sea. *Petroleum Geoscience*, **4**, 67-80.

Hansen, 1996. Quantification of net uplift and erosion on Norwegian Shelf south of 66N from sonic transit times of shale. *Norsk Geologisk Tidsskrift*, **76**, 245-252.

Isaksen, D. and Tonstad, K., 1989. A revised Cretaceous and Tertiary lithostratigraphic nomenclature for the Norwegian North Sea, NPD-Bulletin, 5, *Oljedirektoratet, Stavanger report.*

Iijiama, A. 1978. Geological occurrences of zeolite in marine environments. In: Sand, L.B. and Mumpton, F.A. (Eds.) *Natural Zeolite: Occurrence, properties, use*. Pergamon, Oxford, 175-198.

Kastner, M. and Stonecipher, S.A. 1978. Zeolites in pelagic sediments of the Atlantic, Pacific and Indian Oceans. In: Sand, L.B. and Mumpton, F.A. (Eds.) *Natural Zeolite: Occurrence, properties, use*. Pergamon, Oxford, 199-218.

Ming, D.W. and Dixon, J.B. 1987. Technique for the separation of clinoptilolite from soils. *Clays and Clay Minerals*, **35**, 469-472.

Moore, D.M. and Reynolds, R.C. 1997. *X-Ray Diffraction and the Identification and Analysis of Clay Minerals, Second Edition.* Oxford University Press, New York.

Mumpton, F.A and Ormsby, W.C., 1976. Morphology of zeolites in sedimentary rocks by scanning electron microscopy. *Clays and Clay Minerals*, **24**, 1-23.

Nathan, Y and Flexer, A. 1977. Clinoptilolite paragenesis and stratigraphy. *Sedimentology*, **24**, 845-855.

Ogihara, S and Iijama A. 1989. Clinoptilolite to heulandite transformation in burial diagenesis. In: Jacobs, P.A., v. Santen, R.A. (Eds.) *Zeolites, facts, figures, future*. Elsevier, Amsterdam, 491-500.

Ogihara, S. 1994. Ba-bearing clinoptilolite from ODP Leg 127, Site 795, Japan Sea. *Clays Clay Minerals*, **42(4)**, 482-484.

Reynolds, R.C. and Reynolds, R.C. 1996. Description of Newmod-for-Windows™. The calculation of one-dimensional X-ray diffraction patterns of mixed layered clay minerals.

Riis, F and Fjeldskaar, W. 1992. On the magnitude of the Late Tertiary and Quaternary erosion and its significance for the uplift of Scandinavia and the Barents Sea. In R.M. Larsen, H. Brekke, Larsen, B.T. and Talleras E., (eds.) Structural and tectonic modelling and its application to petroleum geology, Norsk Petroleums Forening, *NPF Special Publication*, **1**, 163-185.

Rundberg, Y. 1989. Tertiary sedimentary history and basin evolution of Norwegian North Sea between 60°N-62°N, an integrated approach. Dr. ing. Thesis, Universitetet i Trondheim, Norges Tekniske Høgskole, Institut for Geologi og Bergteknikk, Norway, 292 pp.

Stonecipher, S.A. 1978. Geochemistry and deep-sea phillipsite, clinoptilolite and host sediments. In: Sand, L.B. and Mumpton, F.A. (Eds.) *Natural Zeolite: Occurrence, properties, use*. Pergamon, Oxford, 221-234.

Vanucci, S. Pancini, M.G., Vaselli, O. Coradossi, N. 1992. Presence of clinoptilolite in the Maarstrichtian pelagic sediments of the Barranco del Gredero Section (Crarvaca, S-E Spain). *Chemical Erde* **52**, 165-177.

Figure 1: 1 m sandstone core from the Utsira Formation, well 15/9-A-23.

Figure 2: Schematic plan of the 1 metre core identifying sample locations.

Core plan and sampling strategy for Utsira Formation

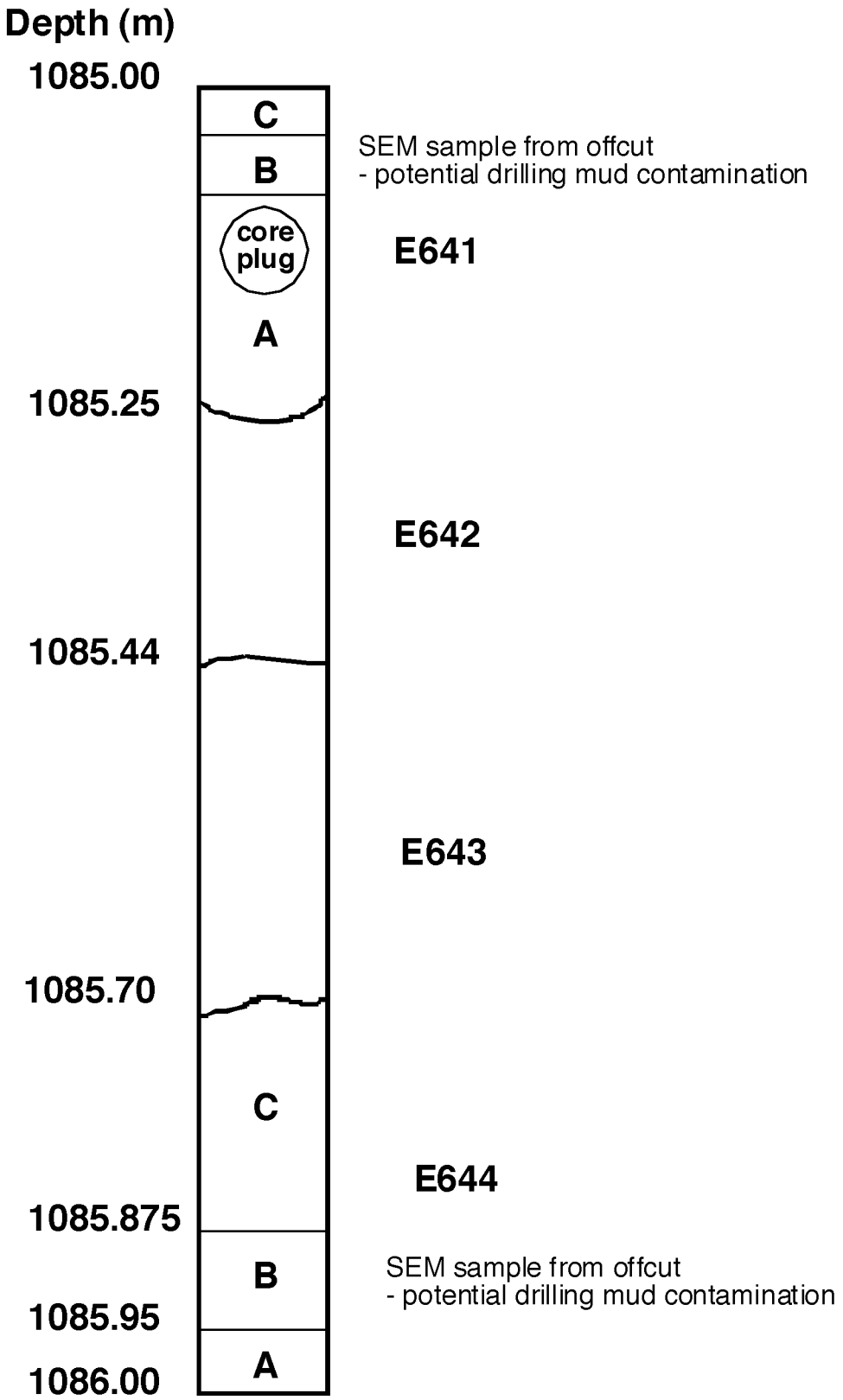

Figure 3: Schematic flowsheet describing the modal analysis methodology employed.

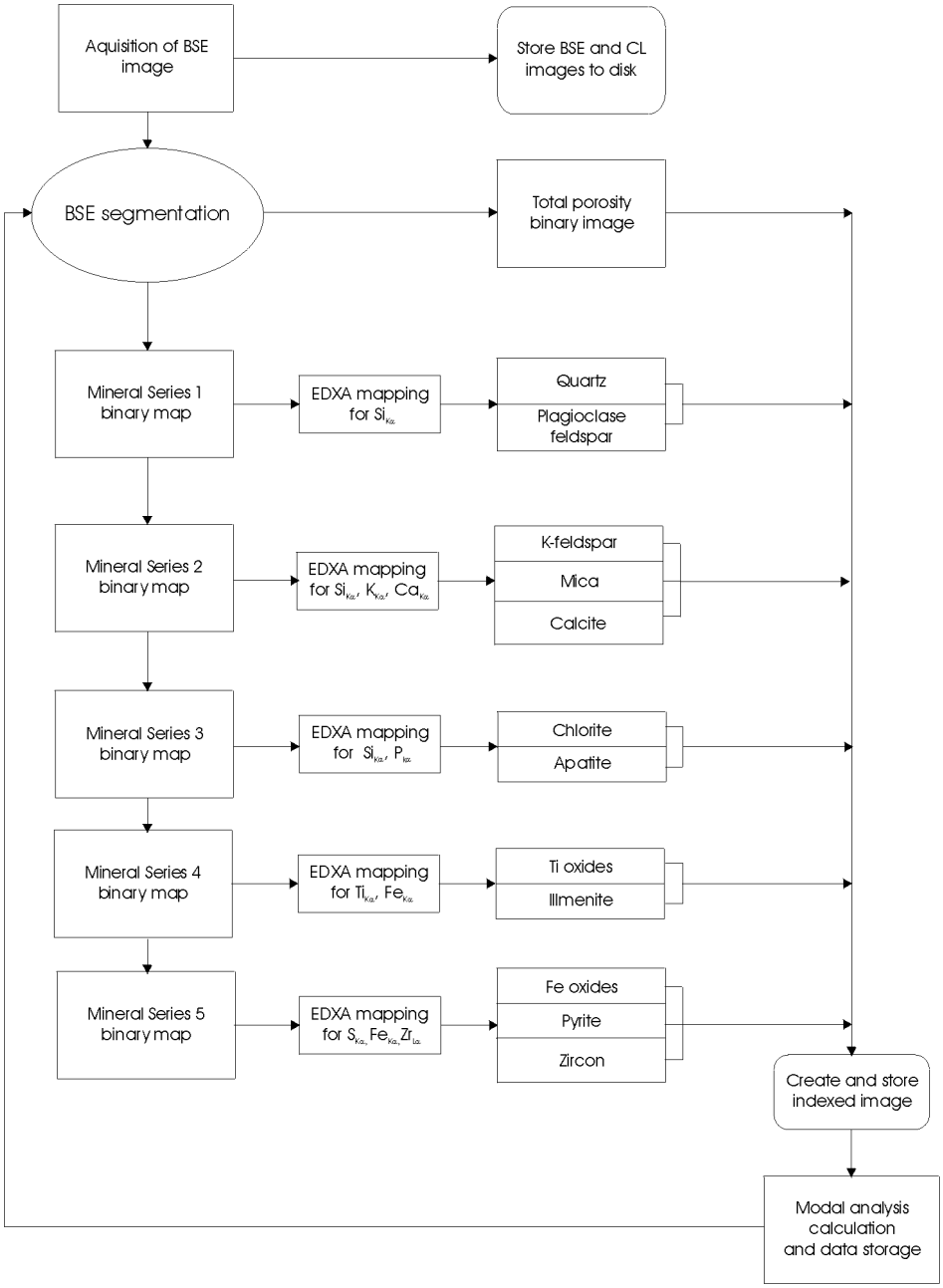

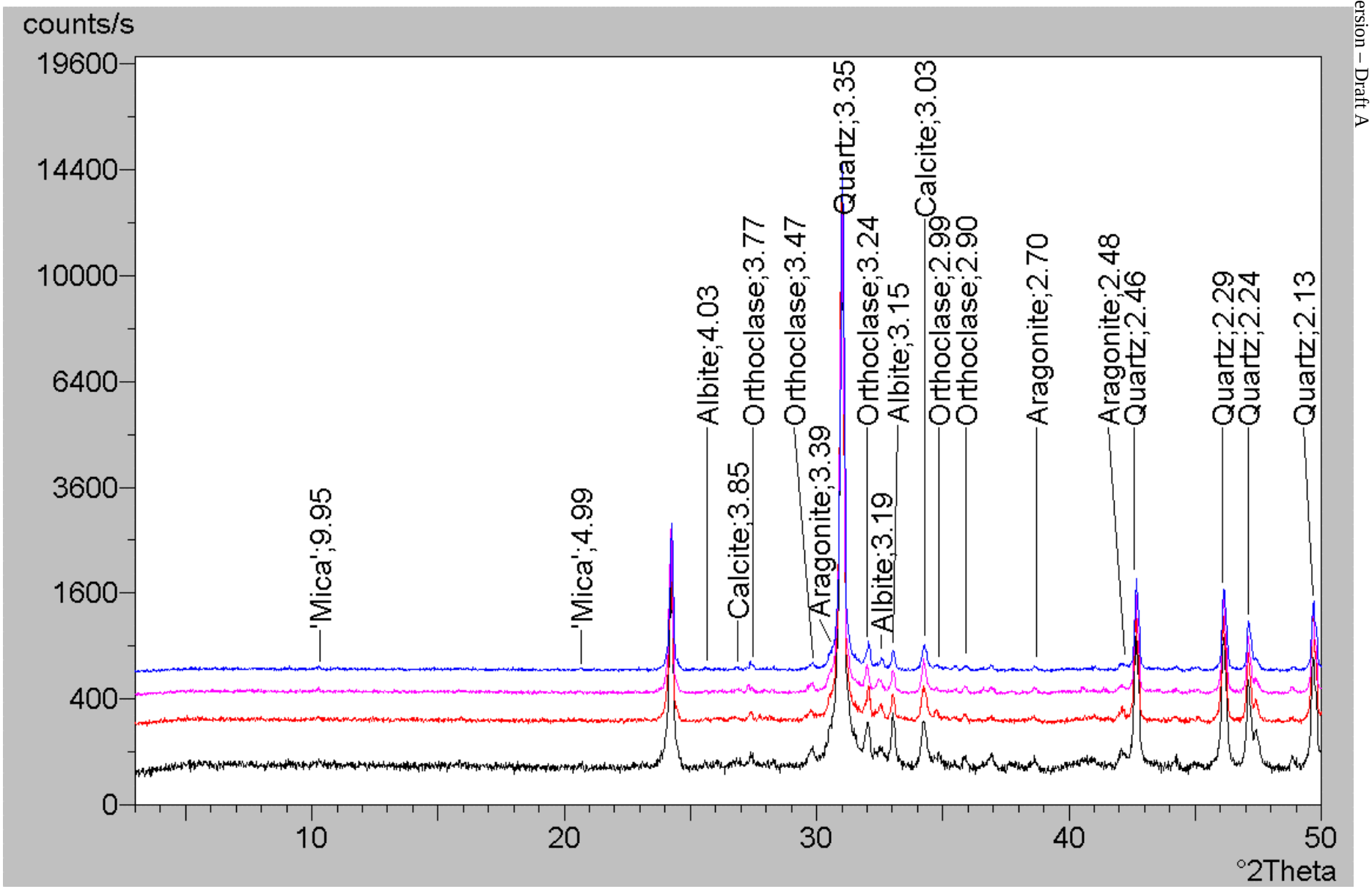

Figure 4: Whole-rock X-ray diffraction traces for samples E641A (black trace), E642 (red trace), E643 (magenta trace) and E644 (blue trace) showing major peak assignations and d spacings. Co-Ka radiation.

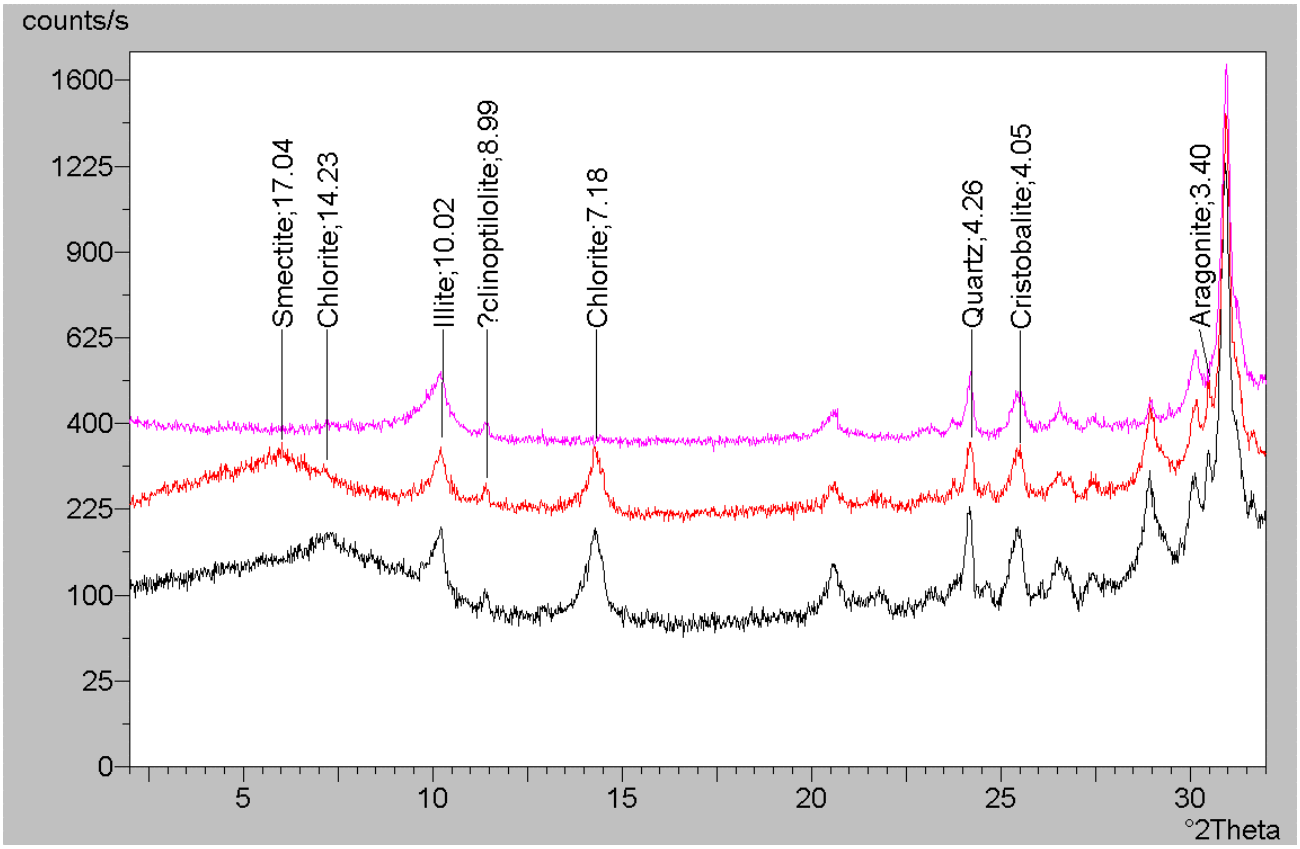

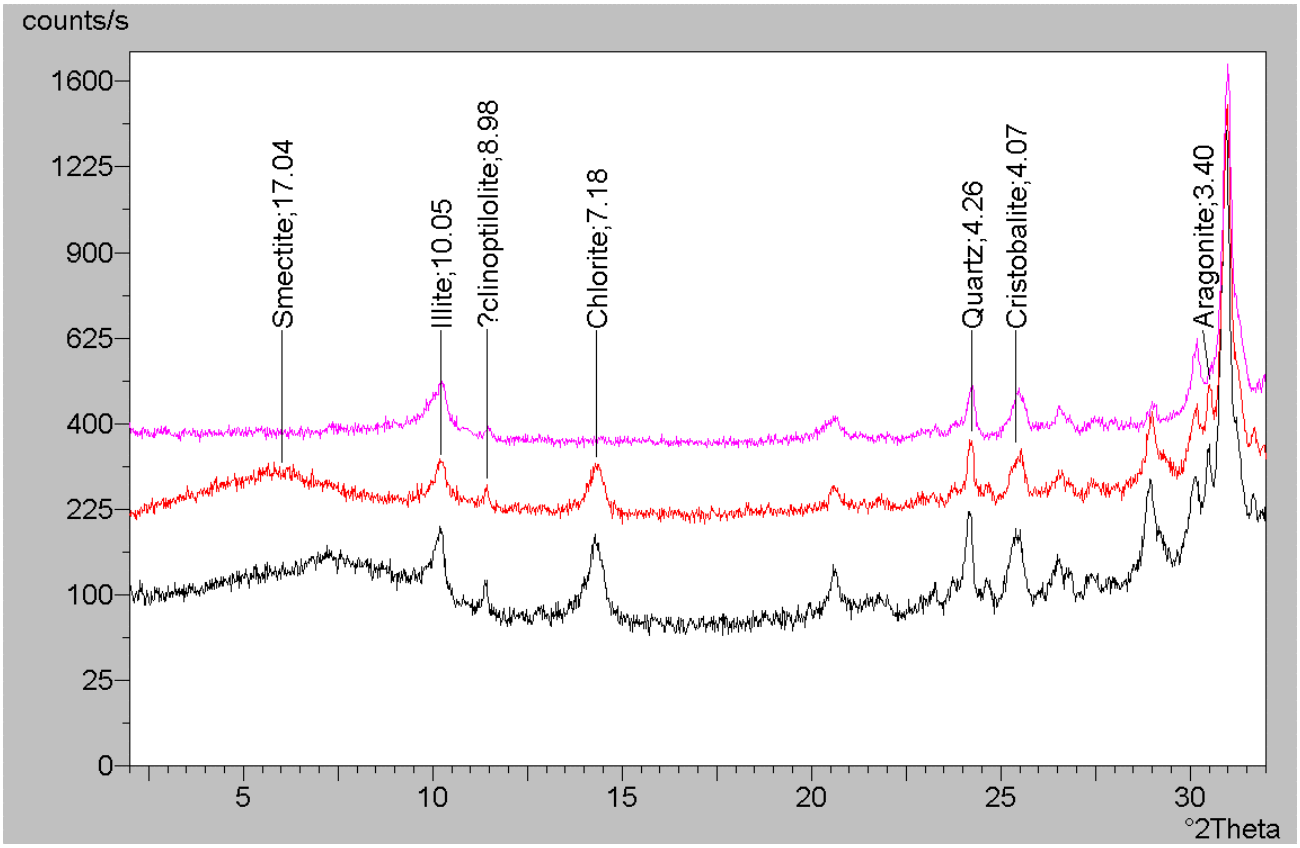

Figure 5: <2 µm oriented mount X-ray diffraction traces (air-dry: black trace; glycol-solvated; red trace, heated 550°C/2 hours; magenta trace) for samples E641A (above) and E642 (below) showing identified minerals and their diagnostic d spacings. Co-Kα radiation.

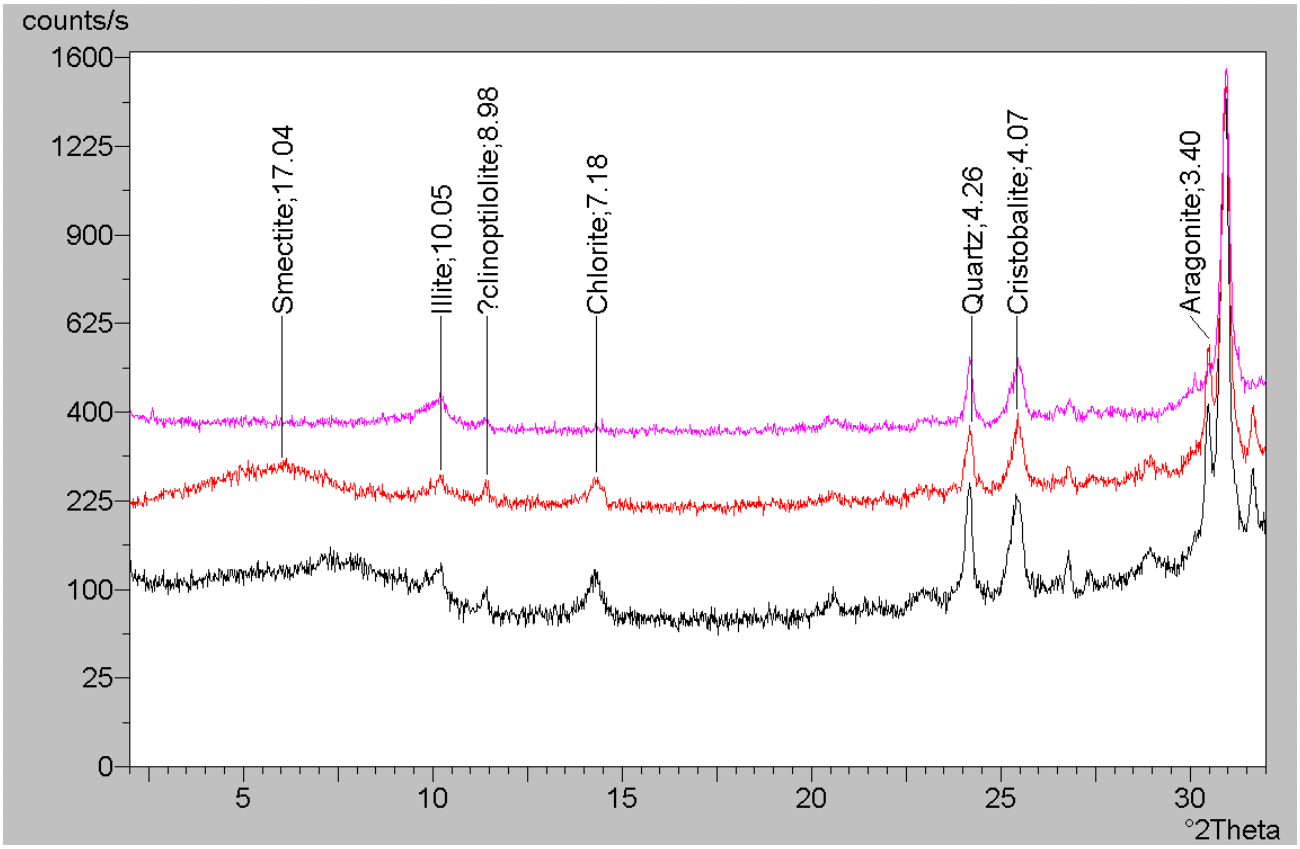

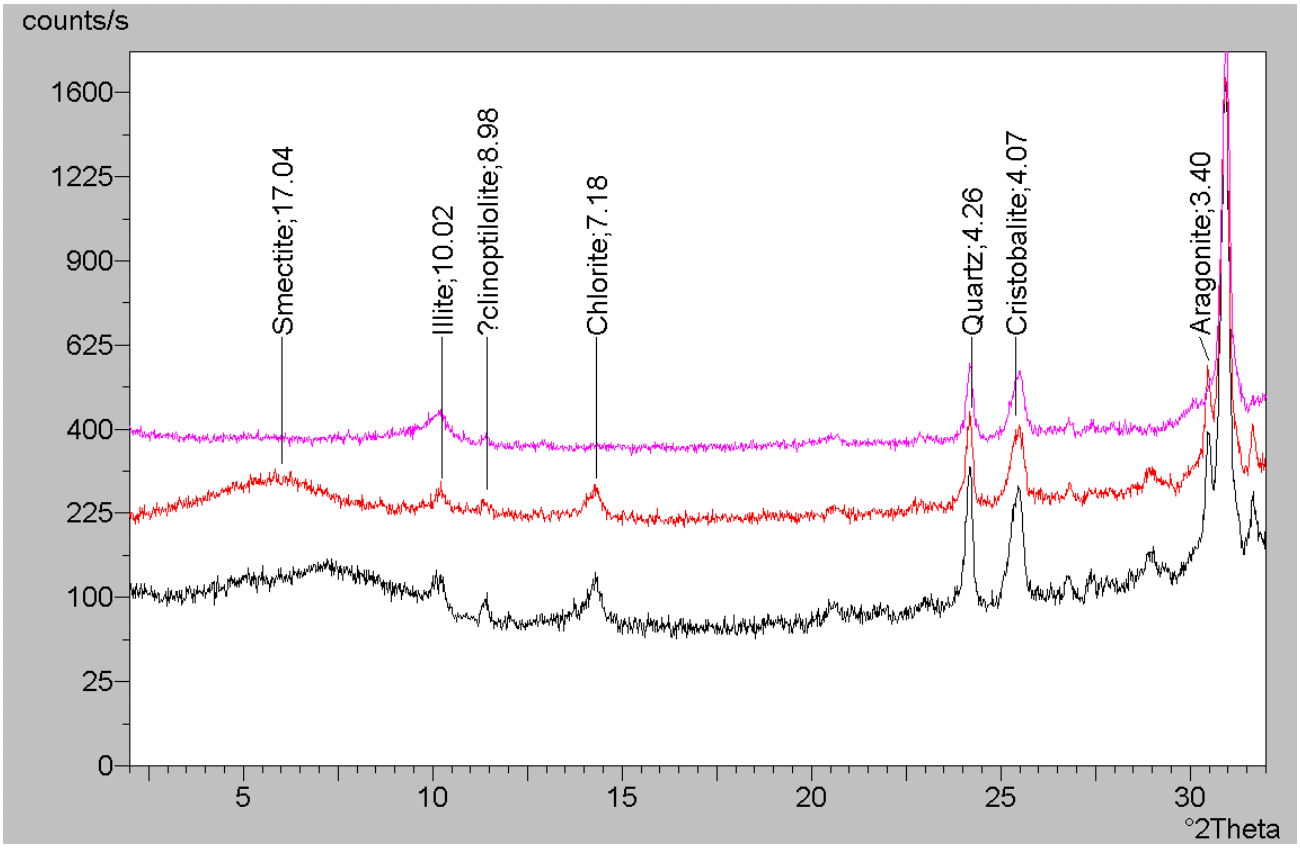

Figure 6: <2 µm oriented mount X-ray diffraction traces (air-dry: black trace; glycol-solvated: red trace, heated 550°C/2 hours; magenta trace) for samples E643 (above) and E644 (below) showing identified minerals and their diagnostic d spacings. Co-Kα radiation.

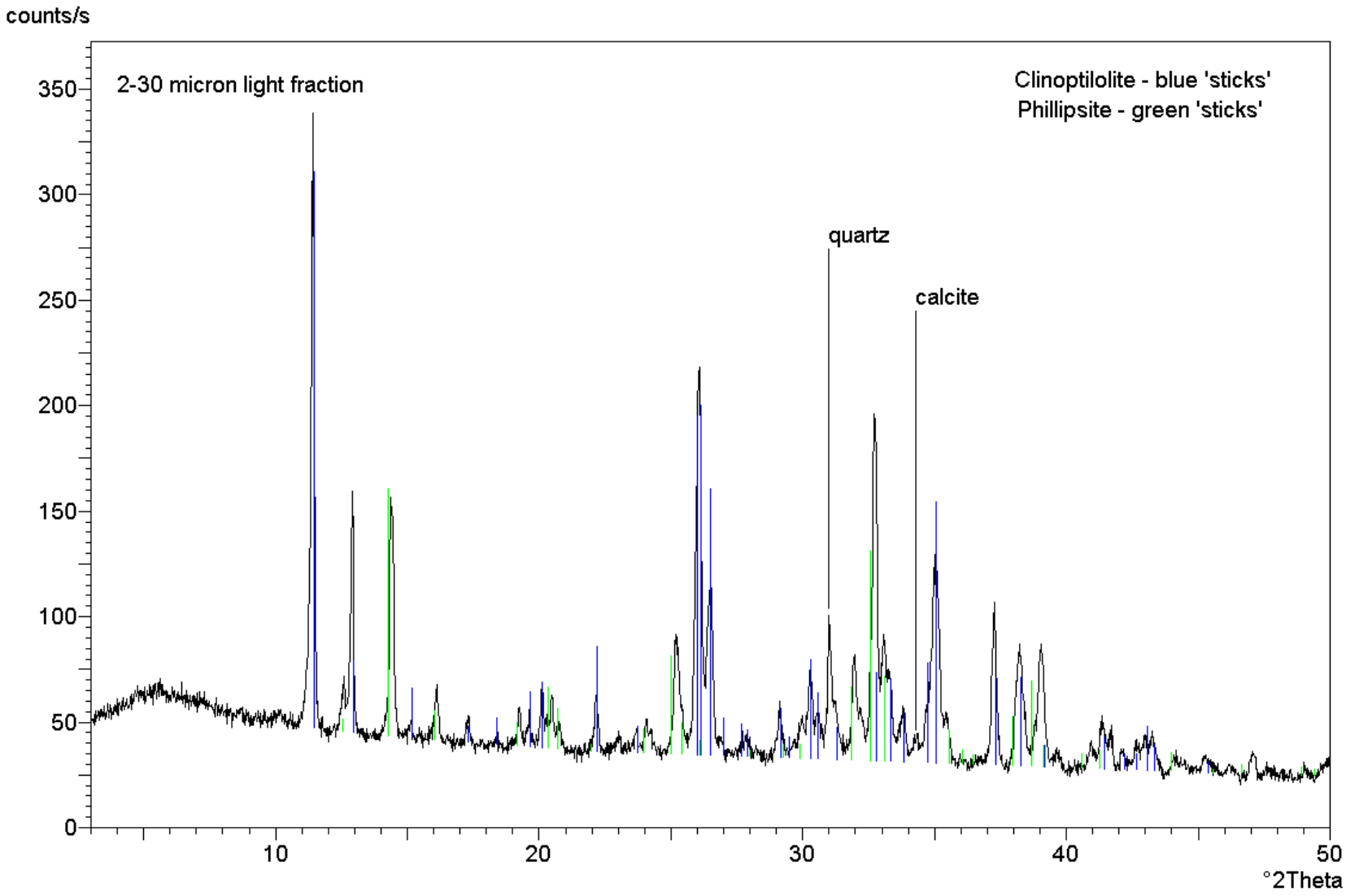

Figure 7: XRD Trace of -30+2 µm 'light' fraction, indicating clinoptilolite and phillipsite.